LANGMUIR Article
Cite This: Langmuir XXXX, XXX, XXX−XXX
pubs.acs.org/Langmuir

Microfluidic Shear Assay to Distinguish between Bacterial Adhesion and Attachment Strength on Stiffness-Tunable Silicone Substrates

Sanya Siddiqui,[†] Arvind Chandrasekaran,[†] Nicholas Lin,[†] Nathalie Tufenkji,[†] and Christopher Moraes*[,†,‡,§]

[†]Department of Chemical Engineering, [‡]Department of Biomedical Engineering, and [§]Rosalind and Morris Goodman Cancer Research Centre, McGill University, Montréal, QC, Canada H3A 0C5

Supporting Information

ABSTRACT: Tuning surface composition and stiffness is now an established strategy to improve the integration of medical implants. Recent evidence suggests that matrix stiffness affects bacterial adhesion, but contradictory findings have been reported in the literature. Distinguishing between the effects of bacterial adhesion and attachment strength on these surfaces may help interpret these findings. Here, we develop a precision microfluidic shear assay to quantify bacterial adhesion strength on stiffness-tunable and biomolecule-coated silicone materials. We demonstrate that bacteria are more strongly attached to soft silicones, compared to stiff silicones; as determined by retention against increasing shear flows. Interestingly, this effect is reduced when the surface is coated with matrix biomolecules. These results demonstrate that bacteria do sense and respond to stiffness of the surrounding environment and that precisely defined assays are needed to understand the interplay among surface mechanics, composition, and bacterial binding.

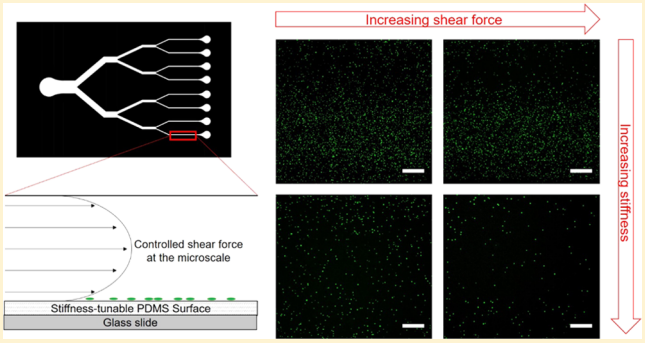

INTRODUCTION

The design of coatings for bioimplantable technologies is a challenging problem that is critical to improve implant functionality, enable host tissue integration, and prevent immune rejection. Coating implantable devices with a layer of extracellular matrix (ECM) proteins, ions, and other growth factors is a well-established strategy to improve cell adhesion and tissue integration.[1,2] Recently, mechanical stiffness has emerged as an important design parameter that may be used to modulate the body's response to an implanted device or material.[3−5] Tissues and organs vary widely in terms of their intrinsic mechanical rigidity,[6,7] and designing medical devices to match the intrinsic tissue stiffness of brain (50 Pa) and bone (1 GPa)[8] tissues, for example, has improved integration into each of these organs.[9] Designing implantable devices with the optimal combination of mechanical rigidity and surface characteristics may hence greatly improve our capacity to engineer implantable systems.

A critically important parameter to consider in implant design is the susceptibility of the device to infection and bacterial growth.[10] Implant-associated infections are initiated by bacterial adhesion to the implant surface and subsequent colonization, ultimately resulting in the formation of drug-resistant biofilms with considerable adverse health effects.[11−15] Treating biofilm-associated implant infections has become increasingly difficult, as biofilms can be strongly resistant to current antibiotic treatment regimens. Limiting the initial adhesion of bacteria, and hence the subsequent formation of biofilms, is thus a critically important design strategy to avoid this life-threatening outcome.[16−20]

Although manipulating the physical properties of implant surfaces could limit rejection, the impact of mechanical stiffness of the interface on bacterial adhesion is not well understood.[21,22] Given the considerable impact of substrate stiffness on mammalian cells,[23−26] it seems likely that bacteria would also be affected by this parameter. Whereas the effects of surface roughness and topography on bacterial attachment and function are well established (reviewed in ref 27), the effect of substrate rigidity on bacterial attachment and retention is limited to relatively few studies (summarized in Table 1).[28−32] These studies do show effects, but no consistent trend has emerged on either porous hydrogels or nonporous solid surfaces. These disparities are perhaps due to variations in stiffness-tunable substrate materials, adhesive coating protocols, and bacterial strains. Finally, variations in assay protocols could generate considerable surface shear stresses that could alter adhesion, or even retention of bacteria on the surfaces, further biasing any observed results.

Given this broad variation in literature results, a technique to distinguish between bacterial adhesion and adhesive strength

Received: March 18, 2019
Revised: June 6, 2019
Published: June 9, 2019

DOI: 10.1021/acs.langmuir.9b00803
Langmuir XXXX, XXX, XXX−XXX

Table 1. Summary of Recent Literature Works Studying the Effect of Mechanical Stiffness on Bacterial Adhesion and Retention, over Various Stiffness Ranges and Substrates

author and reference	substrate	stiffness range	assay technique	results
Guégan et al.[28]	agarose (hydrogel)	6.6−110 kPa	static batch assay	adhesion of *Pseudoalteromonas sp.* D41 increased with higher stiffness. Agglomerated adhesion of *Bacillus sp.* 4J6 on lower stiffness
Kolewe et al.[29]	agar; poly(ethylene glycol) dimethacrylate (hydrogel)	44−6500 kPa	static batch assay	adhesion of *E. coli* K12 correlated positively with increasing hydrogel stiffness
Lichter et al.[30]	polyelectrolyte multilayer film (nonporous)	1000, 10 000 kPa	static and shaking batch assay	adhesion of *Staphylococcus epidermidis* ATCC #14990 and *Escherichia coli* w3100 was positively correlated with increasing stiffness
Song and Ren[31]	poly(dimethylsiloxane) (nonporous)	100−2600 kPa	static batch assay	lower substrate stiffness promoted attachment and growth of *E. coli* RP437 and *Pseudomonas aeruginosa* PA01
Wang et al.[32]	polyacrylamide (hydrogel)	0.017−0.654 kPa	microfluidic shear assay	adhesion of *Staphyloccocus aureus* AH2547 decreased with increasing stiffness

could resolve this conflicting information. An ideal system to study this phenomenon would create robustly reproducible, laminar flow conditions over candidate substrates of interest and would additionally allow experimental scale-up to adequately study a wide variety of bacteria and experimental conditions that will influence bacterial adhesion. Parallel plate flow chambers may be suitable, but limited control over chamber dimensions would require large sample volumes for shear experiments, and may not provide adequate control over wall shear stress when testing soft materials that are prone to deflection during pressurized flow. Furthermore, the large system size introduces several sources of error in applied shear stress, including pressure-driven substrate deformation and delivery tube fluidic capacitance. Microfluidic flow systems provide a suitable alternative to these systems, as confined laminar flow is robustly reproducible, spatially homogeneous, and applied shear stresses are easily controlled.[33−39] Furthermore, microscale fluidic channels allow scaled-up experimentation to test the effects of several surface modifications on the same bacterial strain, from a single sampled population. Well-controlled experiments possible with an appropriately designed microfluidic shear assay may hence allow greater insight into bacterial adhesion behavior on candidate implantable coating materials.

In this work, we designed and fabricated a microfluidic shear assay to understand the combinatorial effects of substrate material stiffness and ECM protein coatings on bacterial attachment and retention. To modify substrate stiffness in a material relevant for implantation studies, we integrated silicone encapsulant materials of varying stiffness[40] as a substrate in the microfluidic devices. Stiffness-tunable formulations of poly(dimethylsiloxane) (PDMS) are widely used as a coating to insulate electrode arrays, particularly in neural and cochlear implants,[41,42] and can be mechanically tuned over several orders of magnitude. Furthermore, the nonporous, optically flat, neutrally charged surfaces of this material provide a well-controlled and characterized surface for such studies. To benchmark this simple device against existing standard adhesion assays that do not provide tight control over shear stress conditions, we first conducted a stirred-batch adhesion assay to study bacterial attachment on soft and stiff PDMS substrates. We then measured bacterial adhesion and retention using the microfluidic platform with controlled applied shear stress and protein surface modifications. Our results demonstrate that the mechanical properties of the substrate play a significant role in bacterial retention, but not initial bacterial adhesion, and that control over applied shear is critically important to understand the interplay among substrate mechanics, surface composition, and bacterial binding. The developed technique may hence have broad utility in understanding and identifying candidate silicone coating materials for various implantation applications.

MATERIALS AND METHODS

Bacterial Cell Culture. A stock culture of fluorescently tagged *Escherichia coli* K12 (Gram negative, nonpathogenic) was used in the experiments and maintained at −80 °C in Luria−Bertani (LB; Fisher, Cat No. 12795027) broth supplemented with 30% glycerol. A sterile inoculation loop was used to inoculate an LB agar plate from the frozen stock culture, and the agar plate was incubated at 37 °C overnight and stored at 4 °C. For each experiment, a single colony from a fresh plate (maximum 2 week old) was used to inoculate 5 mL of LB broth in a 15 mL centrifuge tube. The inoculated medium was incubated at 37 °C for 20 h in a shaker operating at 150 rpm (Labnet, 311DS). The overnight culture was vortexed and then centrifuged for 5 min at 7164*g* (Thermo Fisher, Heraeus Multifuge X3R). In a biological safety cabinet, the supernatant was decanted and the pellet was resuspended in 5 mL of sterile phosphate-buffered saline (PBS; Fisher, Cat No. SH3025601). Centrifugation and resuspension were repeated one additional time to remove traces of growth medium and metabolites. The concentration of the cell suspension was determined by measuring the optical density (OD) at 600 nm in a UV−visible spectrophotometer (Thermo Fisher, BioMate 3 S). The suspension was diluted in PBS to a final OD of 0.20 (corresponding to a cell concentration of $\sim 10^6$ cells/mL).

Preparation of PDMS Substrates with Variable Stiffness. Sylgard 184 silicone elastomer kit (Dow Corning) was used to prepare the stiff PDMS substrates. A standard ratio of 1:10 (curing agent to elastomer base) was mixed thoroughly in a weigh boat. The soft PDMS substrates were prepared using Sylgard 527A&B dielectric gel (Dow Corning). In a weigh boat, parts A and B were mixed thoroughly in a standard 1:1 ratio. Both PDMS mixtures were degassed in a desiccator to remove air bubbles. For the batch adhesion assay, the mixtures were evenly spread onto 18 mm round, acetone-cleaned coverslips (Fisher, Cat no. 12-545-100) using a spin coater (1000 rpm for 60 s; Laurell Technologies, model no. WS-650MZ-23NPPB). For the high-throughput microfluidic adhesion assay, the mixtures were coated onto 75 mm × 50 mm acetone-cleaned glass slides (Fisher, Cat no. 12-553-5B) using the same settings. PDMS-coated glass slides were then cured at 70 °C overnight to allow for full polymer cross-linking. The PDMS-coated coverslips were cured onto the bottoms of a 12-well plate (Fisher, Cat no. 12-556-005). A drop of uncured PDMS was dispensed onto the bottom of each well. The coverslips were then gently placed on top and cured overnight at 70 °C to ensure the samples remained fixed in place while performing the batch adhesion assay.

DOI: 10.1021/acs.langmuir.9b00803
Langmuir XXXX, XXX, XXX−XXX

Shear Rheology Measurements. The stiffness of the PDMS samples was characterized using a strain-controlled shear rheometer (Anton-Paar, MCR 302). Soft and stiff PDMS samples were cured onto 12 mm acetone-cleaned glass coverslips, as described above. The samples were securely fixed onto the bottom plate of the parallel plate rheometer using double-sided adhesives. The storage modulus of each sample was measured at 10% strain and an angular frequency of 10 s^{-1}.

Preparation of ECM Solutions. A collagen solution was prepared using a 5 mg/mL collagen type I, bovine stock (Life Technologies, Cat no. A10644-01). Acetic acid (Sigma, Cat no. 320099) was diluted in deionized water to a concentration of 0.02 N and subsequently syringe-filtered (Fisher, Cat no. 09719 C) in a biological safety cabinet to ensure sterility. The collagen stock was diluted in the acetic acid solution, ensuring solubilization of the collagen protein, to a desired concentration of 25 μg/mL. A fibronectin solution was also prepared to the same concentration of 25 μg/mL using a 1 mg/mL human fibronectin stock (Sigma, Cat no. FC010-5MG) diluted in sterile PBS (Fisher, Cat no. SH3025601). A 1:1 combination solution was prepared by mixing equal portions of the collagen and fibronectin solutions.

Batch Adhesion Assay. Two 12-well plates fixed with PDMS-coated coverslips, as previously described, were used in the batch adhesion assay. Each well plate contained six wells of stiff PDMS samples and six wells of soft PDMS samples. The samples were fixed onto the bottom of the wells using PDMS as a glue. The plates were sterilized in germicidal UV light for 30 min before ECM coating. A bacterial cell suspension of *E. coli* K12 was prepared as outlined, and 1 mL of the suspension was dispensed into each well and incubated for 2 h. One plate was incubated in static condition at 37 °C, whereas the other plate was incubated on a shaker at 180 rpm, 37 °C to impart shear stress on the samples. Following the incubation, the samples were carefully washed with sterile PBS three times using a pipette, ensuring that the samples were never exposed to air and the surface remained covered in liquid after the washing.

Microfluidic Device Fabrication. A branched microfluidic device was fabricated using standard SU-8 photolithography and PDMS replica molding methods. A master mold was first created using a SU-8 2075 photoresist (MicroChem). A sonicated, acetone-cleaned glass slide (75 mm × 50 mm) was plasma-oxidized for 1.5 min (Plasma Etch Inc., model PE-25) to maximize adhesion of photoresist onto the glass slide. The photoresist was then spin-coated onto the slide at 2000 rpm for 30 s to correspond to a 100 μm height of the master mold. The SU-8-coated glass slide was soft-baked at 70 °C for 10 min and at 100 °C for 15 min. The slide was covered with a mask of the branched device design (CAD/ART Services) and flood-exposed with UV light (Honle UV Technology, Bluepoint UV) for 30 s to polymerize the device design onto the photoresist. Following UV exposure, the slide was postbaked at 70 °C for 5 min and at 100 °C for 20 min. The remaining unpolymerized photoresist was removed using the SU-8 developer (MicroChem) for 15 min. The resulting structures were flood-exposed with UV light again for another 15 min to ensure complete cross-linking.

The master mold was exposed to trichlorosilane (Gelest, Cat no. SIT8174.0) vapors in a desiccator, connected to a vacuum line, to prevent substrate adhesion during replica molding. The device features were replica-molded using PDMS from the silanized master mold. The PDMS prepolymer base and cross-linking curing agent were well mixed in a 10:1 weight ratio and degassed in a desiccator until air bubbles were removed from the mixture. The SU-8 master was placed in a large weigh boat, and the PDMS mixture was carefully poured on top and degassed again. The PDMS-covered master mold was then cured at 70 °C for a minimum of 1 h. The PDMS mold was peeled from the SU-8 master, and excess PDMS was trimmed.

Device Bonding. The PDMS replicate of the flow device was biopsy-punched with a 2 mm punch at the inlet and outlet ports of the device channels. The PDMS-coated glass slides, described earlier, were bonded to the replicate as the bottom substrate using oxygen plasma bonding. Both pieces were plasma-oxidized for 1.5 min, and the replicate was carefully placed on top of the glass slide. The bonded device was then placed in an oven at 70 °C for 10 min to complete the bonding process and return the exposed PDMS surfaces to their native state. Before use, the devices were UV-sterilized for 30 min in a germicidal UV chamber.

Device Flow Characterization. Green fluorescent beads (FSDG006, Bangs Laboratories Inc.) of mean diameter 4 μm in a stock concentration of ~40×10^6/mL were diluted in reverse osmosis water and loaded into a 10 mL syringe (Beckton Dickinson, Canada). The syringe was then attached to a syringe pump (Med Fusion Systems, model 1001), and the microfluidic tubing (Cole-Parmer, Cat no. EW-06417-21) connected to the syringe was press fit into the inlet port of the microfluidic device. The device was positioned and firmly held under a fluorescence microscope (Olympus IX-73). The channels were initially primed with liquid at a high flow rate (1 mL/min) to ensure continuous flow in all of the channels without any leaks. Movement of fluorescent beads was tracked with a microscope at the required experimental flow rates (0.01, 0.05, and 0.1 mL/min) using a streakline imaging technique. Three different images were recorded at a low camera shutter speed (1 s) such that the streamlines followed by the beads in each of the channels appeared as fluorescent streaks. The longest streak observed in approximately the center of each of the channels was used to compute the characteristic flow velocity.

Shear Stress Calculations. The shear stress acting on the bacteria in the microfluidic channels was calculated. The parallel plate approximation uses the shear viscosity of the fluid, the volumetric flow rate, and the channel dimensions to calculate the wall shear force. Shear stress in the microfluidic channels was calculated based on methods outlined by Young et al. using a microchannel approximation[43] (eq 1) that incorporates a multiplication factor onto the parallel plate approximation, based on the aspect ratio of the channel (eqs 2 and 3). Using the parallel plate and microchannel approximations, the wall shear stress can be described as

$$\tau_w = \frac{6\mu Q}{wh^2}\left(\frac{m+1}{m}\right) \tag{1}$$

where

$$m = 1.7 + 0.5\alpha^{-1.4} \tag{2}$$

for

$$\alpha = \frac{h}{w} < \frac{1}{3} \tag{3}$$

in which τ_w is the wall shear stress, μ is the fluid viscosity, Q is the volumetric flow rate, h and w are the heights and widths of the microfluidic channel, and α is the aspect ratio of the microfluidic channel.

Finite Element Modeling of Channel Deformation. Deformation of the microchannel by fluid pressure was modeled numerically with COMSOL v.5.3 (Comsol Inc., Burlington, MA). The glass slide, thin stiffness-tunable PDMS layer (75 μm), and the Sylgard 184 PDMS microfluidic channel (100 μm height, 600 μm width) were simulated using a two-dimensional, multimaterial geometry with pressure boundary loads. A normal pressure load was applied on all interior surfaces of the fluidic channel to deform the surrounding material. Both PDMS types were formulated as incompressible (Poisson's ratio ν = 0.49), with experimentally obtained modulus values. Parameters for the glass substrates were obtained from the built-in COMSOL library of materials ($E = 7.31 \times 10^7$ kPa; ν = 0.17).

High-Throughput Shear Flow Assay. The channels of the microfluidic device were first functionalized with ECM solutions of collagen, fibronectin, and a combination of collagen and fibronectin at the same concentration (25 μg/mL). The preparation of the ECM solutions is described earlier in the Materials and Methods section. The desired solution (1.25 μL) was injected into the outlet port of the microfluidic channels. Channels 1 and 2 were not coated and left as controls. Channels 3 and 4 were coated with collagen, channels 5 and 6 were coated with fibronectin, and channels 7 and 8 were coated with the combination solution. The ECM solutions were incubated onto

DOI: 10.1021/acs.langmuir.9b00803
Langmuir XXXX, XXX, XXX−XXX

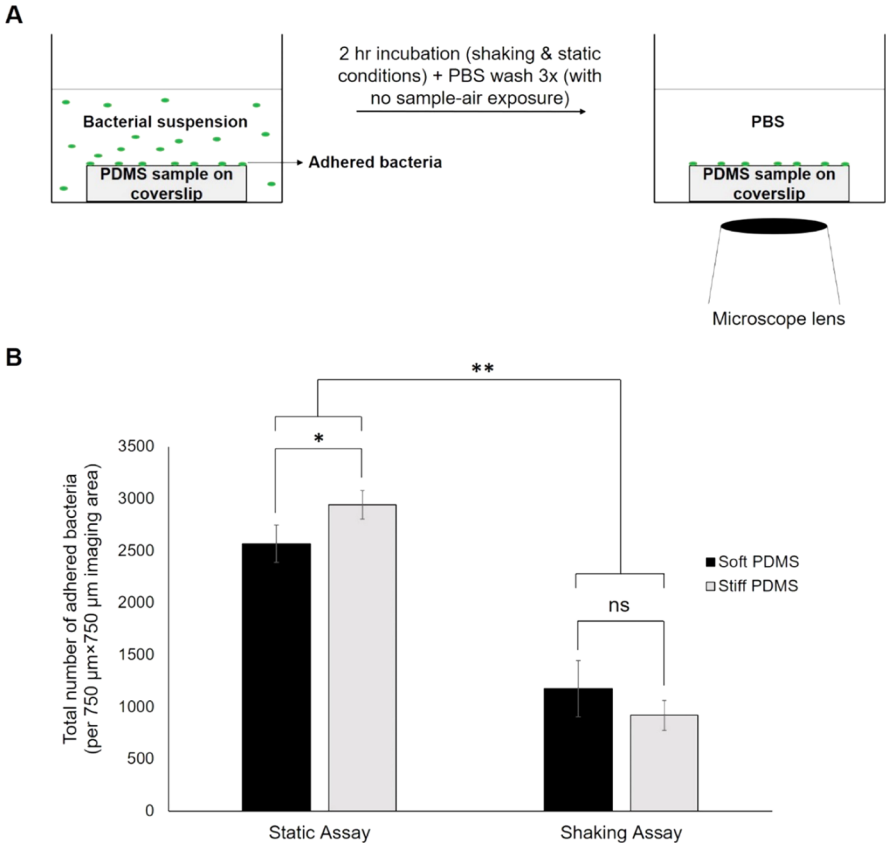

Figure 1. (A) Schematic of the batch adhesion assay methodology. Samples are incubated in a bacterial suspension (in both shaking and static conditions) and subsequently washed with PBS (with no liquid−air exposure). Adhered bacteria are imaged by fluorescence microscopy. (B) Average bacterial attachment in the shaking and static adhesion assays. The total number of adhered bacteria is higher on the samples of the static assay compared to that of the shaking assay. There was also statistically distinct adhesion between the soft and stiff samples in the static adhesion assay alone. Error bars on the graph represent standard deviation among the replicates (*$p < 0.05$, **$p < 0.001$ by two-way ANOVA, $n = 3$).

the channel surface for 1 h at room temperature to allow for protein adsorption and subsequently washed with sterile PBS (∼1 mL) injected from the inlet port of the device. Uniform coating was verified by indirect immunostaining and fluorescent labeling of the adhered ECM (data not shown). Microfluidic tubing (Cole-Parmer, Cat no. EW-06417-21) was connected to the inlet port of the device and attached to a syringe through an 18 gauge 1 in. blunt needle (Jensen Global, Cat no. JG18-1.0X). The devices were washed by injecting sterile PBS through a 10 mL syringe, ensuring no air bubbles were present in the channels. Following the wash, the bacterial suspension was injected into the device using a separate syringe and tubing, attached to a syringe pump (Med Fusion Systems, model 1001) at a flow rate of 0.01 mL/min for 15 min. The liquid accumulated at the outlet ports was wiped away with a KimWipe. On the same sample, the flow rate of PBS was increased to 0.05 mL/min for 15 min and finally to 0.1 mL/min for 15 min again.

Imaging and Statistical Analysis. Images of bacteria attached to the substrates were taken on an Olympus IX-73, equipped with a confocal disc spinning unit and a sCMOS camera. Ten viewfields at 40× were captured from random locations on the substrate surface for each sample in the batch adhesion assay. Five viewfields at 10× were captured from random locations on the substrate surface along each channel in the microfluidic flow assay. All experiments were completed in at least triplicate samples. The images of the bacterial cells were exported onto FIJI (NIH) software, and the cell count was determined using the "Analyze Particles" feature. For the statistical analysis of the data, SigmaStat 3.5 software was used with a two-way analysis of variance (ANOVA) test. The overall significance level of the data is indicated on each graph.

RESULTS AND DISCUSSION

PDMS Substrate Characterization. PDMS surfaces of two stiffnesses were readily fabricated into coupons for standard batch adhesion assays and integrated into microfluidic channels for shear-controlled adhesion assays. Tests for leaks under pressurized syringe pump flow demonstrated that the seal between microfluidic channel and PDMS surface was complete. The shear moduli of the soft and stiff substrates were determined to be $G = 0.26 \pm 0.01$ and 124 ± 36 kPa, respectively, by shear rheometry, demonstrating the capability of this system to span a large physiological range of mechanical rigidities.

Static vs Shaking Batch Adhesion Assay. To establish a baseline consistent with other studies, we performed a standard batch adhesion assay, in which PDMS samples were affixed to the bottom of a 12-well plate and incubated in a bacterial suspension of *E. coli* K12 with and without applied shaking (Figure 1A). This strain of bacteria was selected as it is a commonly used model organism for many bacterial assays and can be easily labeled fluorescently to facilitate quantification.

In the standard batch assay experiments we conducted, more bacteria adhered to the stiff substrates under static adhesion conditions, suggesting that rigid surfaces increase bacterial attachment ($p < 0.05$; Figure 1B). However, when cultures were shaken during the experiment, overall adhesion was lower than in the static case, and there was no significant difference in adhesion observed on the two stiffnesses. We had originally

DOI: 10.1021/acs.langmuir.9b00803
Langmuir XXXX, XXX, XXX−XXX

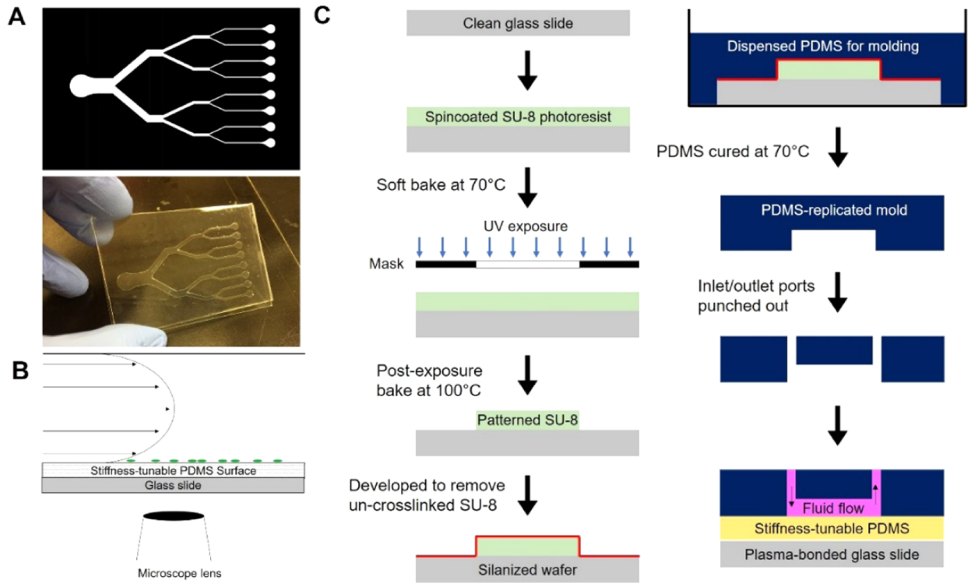

Figure 2. (A) Mask used to fabricate the branched microfluidic device via SU-8 photolithographic processing and a sample microfluidic shear device. (B) Schematic of the cross section of a channel in the shear flow device. (C) Schematic of the photolithography and PDMS replica molding/bonding steps to fabricate the device.

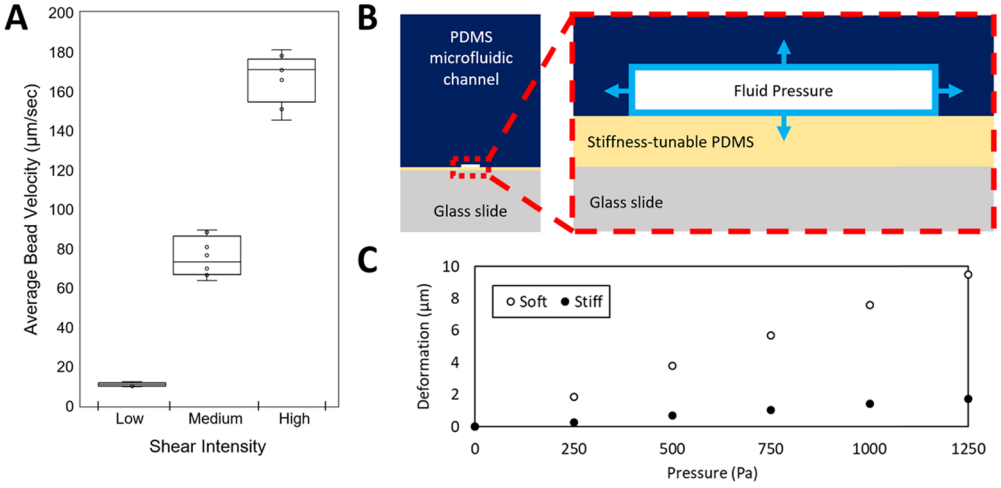

Figure 3. Characterization of shear stress in microfluidic channels. (A) Average bead velocity in each of the eight microfluidic channels at varying flow rates, corresponding to low, medium, and high shear intensities. The box plots denote the median and interquartile range, whereas whiskers indicate the range, with overlaid individual data points. (B) Schematic of finite element simulation to characterize channel deformation under pressurized flow. (C) Simulated change in channel dimensions for expected pressures in the microfluidic shear channels. Based on these simulations, shear stress is expected to be within 10% of nominal values based on deformation of the channel.

expected that shaking would increase the likelihood of bacterial collision and initial attachment to the surfaces and that there would be a predominant effect of surface stiffness on bacterial adhesion. Instead, these results suggest that initially adhered bacteria are being sheared off the surface by turbulent flows during shaking incubation despite the underlying difference in surface stiffness, suggesting that shear forces in culture have significant effects on the outcomes of standard adhesion assays.[44]

These results are consistent with the idea that initial bacterial adhesion is mediated by a reversible physical process that occurs independently from molecule-specific attachment.[45] Although several different factors and environmental conditions are known to affect bacterial adhesion, flow conditions are known to be an important parameter that strongly influences bacterial attachment and detachment during the initial attachment stage.[46−48] In the shaking culture experiments described here, samples are exposed to turbulent fluid flow and large variations in shear stress over time and space as they are simultaneously attaching and detaching from the surface. Even the so-called "static" culture conditions are exposed to uncontrolled shear stresses during wash and rinse steps, which may influence the observed results. Elevated bacterial sensitivity to shear stress at the initial adhesion stages would hence make it extremely challenging to draw conclusions from these relatively crude assays for adhesion to stiffness-tunable substrates. Resolving shear-related factors may hence lead to greater insight into how bacteria interact with surfaces of tunable mechanical stiffness and may explain why the literature on bacteria-substrate stiffness interactions is conflicted.

DOI: 10.1021/acs.langmuir.9b00803
Langmuir XXXX, XXX, XXX−XXX

Microfluidic Flow Cell Design and Operation. To eliminate the uncertainty around shear stress application in standard batch assays, we conducted an adhesion and retention experiment in custom-designed microfluidic channels that provide precise control over applied shear stress on PDMS surfaces of varying stiffness. Each device features eight test channels of 600 μm width and 100 μm depth, symmetrically branched to ensure consistent flow in each channel[43] (Figure 2). The surfaces of each channel can be independently modified by adding a coating solution from the outlet end and evenly sheared under test conditions by applying flow through the single inlet channel. Using this system, bacteria can be seeded and gently rinsed using slow-flow conditions and actively detached from the substrate by applying controlled shear stresses by increasing the flow rate. The strength of bacterial adhesion to the underlying substrate is reflected in the fraction of the bacterial population remaining on the substrate after a known shear stress is applied. The simple microfluidic design hence enables increased-throughput testing for the combinatorial effects of adsorbed ECM proteins and substrate stiffness on bacterial adhesion and retention.

Three flow rates were selected for the shear stress assay, corresponding to low, medium, and high shear stresses. A simple bead velocity test was performed to determine the experimental variability in flow between each of the channels (Figure 3A and Table 2) at the various flow rates. The flow rates and corresponding shear stresses in each channel were experimentally confirmed to be within 13% of the nominal flow rate for each condition. This error could be due to microscopic variations in thickness of each flow channel but likely reflects velocity measurements at different channel heights.

Table 2. Theoretical Shear Stresses Calculated Based on the Corresponding Flow Rate Using the Microchannel Approximation for Shear

flow rate (mL/min)	shear stress (dyne/cm^2)	nominal intensity
0.01	1.7	low
0.05	8.4	medium
0.10	16.8	high

Alternatively, the experimentally observed variations in fluid flow may also be due to changing channel dimensions due to pressure-induced deformation of the soft PDMS layer. To determine whether this is a significant factor, we first analytically determined the maximum back-pressure due to fluid flow to be ~1.1 kPa in channels of these dimensions (Supporting Information). Finite element simulations of deformation in the soft PDMS layer (Figure 3B) at these maximum pressure values indicate that channels deform by at most ~8 μm (Figure 3C) or 8% of the channel height. These values represent the maximum possible deviation from nominal values and are expected to be smaller closer to the fluid exit port. These values translate to maximal wall shear stress variations of <15% from the nominal stated value. Since this variation is negligible compared to the nominal values for low, medium, and high shear stresses tested (Table 2), together these results demonstrate that flow in each channel and at each assay point is sufficiently similar to ensure equivalency between shear stresses in each of the conditions studied.

Substrate Stiffness Differentially Regulates Bacterial Attachment Strength. The microfluidic shear assay developed here allows precise control of flow to separately assess attachment and retention of bacteria, a distinction that is not always considered in classical adhesion assays.[44,49] Attachment refers to the initial binding of the bacteria to the substrate through physicochemical interactions,[50] whereas retention measures the strength of adhesion between the bacterium and the surface. Both parameters likely play an important role in understanding risk factors for biofilm formation on an implant surface.[44] To determine whether these characteristics are different based on substrate rigidity, a suspension of *E. coli* K12 in PBS was injected into the inlet port of the device at low shear stress using a syringe pump set at low flow rates. Sample injection was done carefully to ensure that no air bubbles were present in the syringe, tubing, or channels. Following bacterial injection and adhesion, sterile PBS was flowed through the microchannel network at low shear stress to clear any weakly attached bacteria and the channels were imaged to quantify attachment. No statistically significant differences were observed in adhesion between the soft and stiff substrates at this low shear flow (Figure 4).

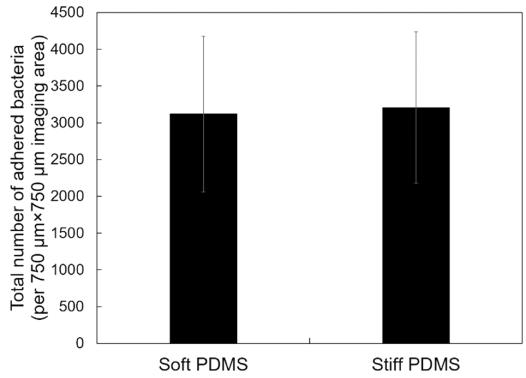

Figure 4. Soft and stiff PDMS substrates were tested in the shear flow assay. The bacterial suspension was flowed into the channels at a low intensity shear force and washed with PBS at the same shear force. The results showed no statistically significant difference between the number of adhered bacteria per unit area of the samples (soft PDMS, 3120 ± 1060; stiff PDMS, 3207 ± 1030; n = 6). Error bars on the graph represent standard error among the replicates.

Increasing levels of shear stress were then applied to the adhered bacteria to determine how tightly they are bound to the surfaces. The number of bacteria remaining adhered under medium and high shear stresses were normalized to the attachment numbers at low shear stress from Figure 4, reflecting the fraction of bacterial cells that are attached strongly enough to the surface to resist controlled application of shear stress. Intriguingly, bacterial retention on soft samples remained relatively constant with the increasing shear stress, indicating sufficient adhesion strength to withstand medium and high shear stresses. In contrast, bacterial retention on stiff samples decreased significantly when applying both medium and high shear stresses (Figure 5). These results indicate that although the initial levels of adhesion between soft and stiff substrates are similar, the binding strength of the adhered bacteria is stronger on soft substrates. These findings do suggest that differences exist in bacterial interactions between soft and stiff silicone substrates, but primarily in the strength of attachment to the substrate, and hence the ability to retain bacteria under flow at the initial attachment stage. Presumably, increased attachment strength will stimulate bacterial pro-

DOI: 10.1021/acs.langmuir.9b00803
Langmuir XXXX, XXX, XXX−XXX

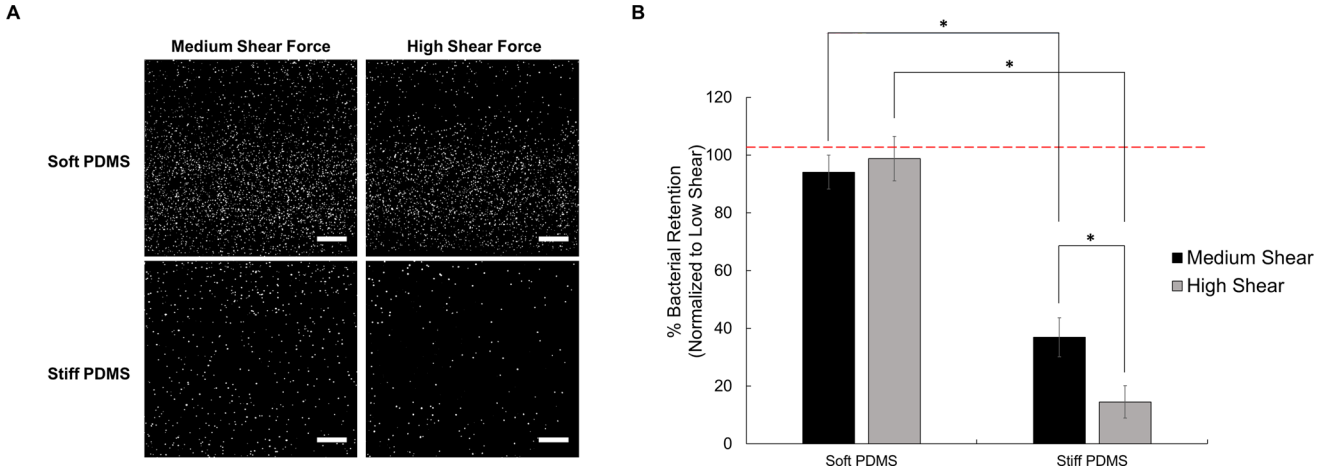

Figure 5. (A) Representative images of bacterial adhesion on PDMS substrates at medium and high flow rates. Scale bar = 100 μm. The images have been converted to black and white for clarity. (B) Bacterial retention of *E. coli* K12 is significantly higher on soft PDMS surfaces at both medium and high shear levels. There was also statistically distinct retention in the stiff samples with the increasing shear level. Results are normalized to the adhesion levels at low shear. Error bars on the graph represent standard error among the replicates (*$p < 0.05$, by two-way ANOVA, $n = 6$).

liferation and biofilm formation and is hence important to consider when conducting such studies.

These results are consistent with findings of Song and Ren[31] that bacteria adhere better to softer silicone surfaces, if we assume that their experiments are really providing a measure of bacterial retention, rather than adhesion as reported in their work. This is quite likely, given that in commonly used adhesion assays adhered bacteria can be exposed to extremely large shear forces during sample handling. For example, Bos et al.[49] demonstrate that the shear forces that accompany movement of an air−liquid interface across the surface, such as during sample transfer between containers, could unintentionally exert large detachment forces up to 10^{-7} N, inadvertently altering study conclusions in a relatively uncontrolled batch-based adhesion experiment. We calculate this force to be equivalent to ∼16 dyne/cm^2 in our microfluidic device channels (our high intensity shear stress condition), which we demonstrate removes a significant portion of the bacterial population. Hence, despite similar initial adhesion profiles, this unintentional shear can generate significant differences between the two substrates, which may substantially alter study conclusions in uncontrolled adhesion experiments.

Our findings for increased retention on soft substrates are also consistent with studies conducted on *S. aureus* adhesion to polyacrylamide hydrogels of tunable stiffness, also performed under flow conditions.[32] Although polyacrylamide has distinctly different physical architectures than those of PDMS (porosity, fibrous architecture, and lower stiffness range), taken together these results do suggest that stiffness is an important parameter to consider to modulate bacterial adhesion and that softer surfaces may be more susceptible to bacterial colonization, despite underlying differences between porous hydrogels and nonporous silicone materials. This limitation hence imposes a lower stiffness limit on the design of implant coatings, to avoid this issue.

Presence of ECM Coatings Reduces Bacterial Attachment Strength on Silicone Substrates. Since ECM coatings are used to promote host tissue integration, and ECM is also deposited on all implanted surfaces by cells in the body, we asked whether a mechanically tuned coating might retain the described bacterial adhesion characteristics once coated with ECM. Soft and stiff silicone encapsulant materials were coated with ECM proteins including collagen, the most abundant protein in the body, and fibronectin, which is commonly associated with foreign body response and fibrotic capsule formation. As a simple proof-of-concept experiment, collagen, fibronectin and a collagen−fibronectin combination were simultaneously tested in the microfluidic devices to determine whether ECM deposition on silicone surfaces affects the observed stiffness-induced differences in bacterial adhesion strength. On soft substrates (Figure 6A), regardless of ECM coating, no statistically significant differences were observed between medium and high shear stresses, but the presence of ECM coatings did reduce the bacterial adhesion strength significantly ($p < 0.05$), as a greater percentage of cells were detached from the surface upon application of medium shear stresses. On stiff substrates however, coating the substrates with collagen alone did not significantly change adhesion strength compared to the control, but incorporating fibronectin into the ECM coating decreased adhesion strength at medium shear stress (Figure 6B). Taken together, this combinatorial study demonstrates that ECM coatings generally reduce the strength of bacterial adhesion on silicone substrates; but this effect is relatively small compared to the stiffness-dependent effects on adhesive strength at medium and high shear stresses.

These results broadly demonstrate the role of surface composition in modulating bacterial adhesion. Here, we found that bacteria binds more strongly to native silicone substrates than to ECM-coated silicones, in a matrix type-dependent manner, as including fibronectin in the coating composition further reduced attachment strength. In contrast with mammalian cells, bacterial attachment to abiotic surfaces is facilitated by both nonspecific hydrophobic and electrostatic interactions,[51] as well as adhesion to proteins and tissues through specific molecular recognition mechanisms such as receptor−ligand or adhesin interactions. Coating silicone surfaces with extracellular matrix proteins may create an inhibitory mechanism, such as steric hindrance, that prevents bacteria from nonspecifically interacting with the silicone substrate.[52−54] Different species and strains of bacteria have

DOI: 10.1021/acs.langmuir.9b00803
Langmuir XXXX, XXX, XXX−XXX

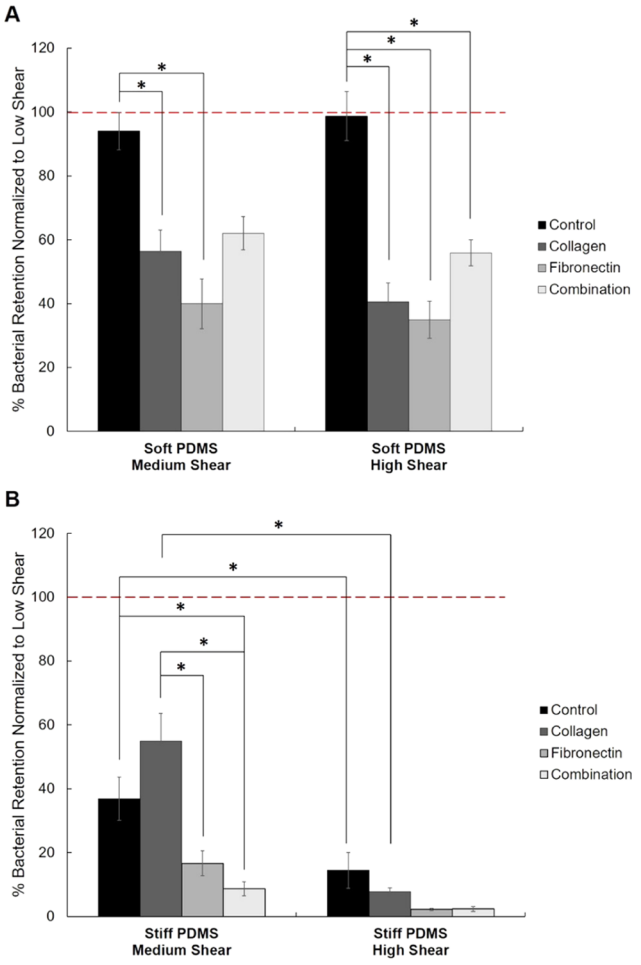

Figure 6. Coating the soft and stiff PDMS substrates with natural ECM molecules generally decreased the adhesion strength of bacteria. The bacterial retention percentage of the substrates at medium and high shear stresses are normalized to low shear stress data. Error bars on the graph represent standard error among the replicates (*p < 0.05, by two-way ANOVA, n = 6).

also been show to exhibit different adhesion mechanisms[53,55] that result in matrix-dependent attachment,[56] further supporting the idea that a balance between nonspecific and specific binding is important for bacterial attachment and colonization. In addition, dynamic receptor-mediated bacterial adhesion to ECM proteins is also mediated by factors including contact area, ligand/receptor density, and shear force.[57,58] For example, the bacterial strain *S. aureus* Phillips is known to adhere to collagen, but this adhesion is highly dependent on applied shear stress.[58] This in turns suggests that bacterial detachment or retention could be significantly altered based on ECM coating composition, further supporting the need for high-throughput methods to evaluate bacterial attachment on combinatorially manipulated substrates.

Given that the in vivo microenvironment consists of many ECM proteins that vary considerably at various implant sites and that infection can occur in multiple bacterial populations, the studies described in this work emphasize the need for high-throughput methods to understand how deposited ECM might influence bacterial adhesion and growth. Overall, we demonstrate that although bacterial adhesion itself is similar across surfaces, the strength of bacterial attachment is modulated by the stiffness of the underlying surface and the type of matrix coating present. These results provide new context in which to clarify conflicting studies in the literature, which indicates that adhesion is greater on both softer surfaces[31,32] and stiffer surfaces.[28−30] In contrast to these previous studies that focus on determining whether bacteria adhere to that surface, our analysis assesses the quality of that adhesion in terms of a physically measurable parameter to better understand how bacteria interact with mechanical stiffness in their surroundings.

CONCLUSIONS

In this work, a microfluidic flow device was engineered to distinguish between adhesion and retention characteristics of bacterial cells to stiffness-controlled substrates. These characteristics were measured on native and protein-coated silicone encapsulant materials to understand the influence of mechanical rigidity of the surrounding environment on bacterial attachment. Our findings demonstrate that although *E. coli* initially adhere in even numbers to both soft and stiff silicones under low shear, a larger fraction of the bacterial cells exhibit stronger adhesion on soft substrates when exposed to high shear. Hence, softer substrates tend to retain bacteria under conditions of external flow. Distinguishing between these two characteristics provides a new context with which to clarify contradictory observations in the literature. When native silicone surfaces are coated with candidate ECM molecules, adhesion strength generally decreased, but these effects were smaller than those of substrate mechanical rigidity. More broadly, the increased-throughput platform developed here enables controlled flow studies over user-selected surfaces, to gain insight into the bacterial colonization process, and may ultimately be used to correlate attachment strength to biofilm formation and potential antibiotic susceptibility. Ultimately, developing high-throughput adhesion assay platforms will facilitate rapid testing of implant materials aimed to initiate host integration while minimizing risk of bacterial infection.

ASSOCIATED CONTENT

Supporting Information

The Supporting Information is available free of charge on the ACS Publications website at DOI: 10.1021/acs.langmuir.9b00803.

Calculations for pressure within microfluidic channels (PDF)

AUTHOR INFORMATION

Corresponding Author

*E-mail: chris.moraes@mcgill.ca.

ORCID

Nathalie Tufenkji: 0000-0002-1546-3441

Christopher Moraes: 0000-0002-8950-2212

Notes

The authors declare no competing financial interest.

ACKNOWLEDGMENTS

This research was supported by funding from the Natural Sciences and Engineering Research Council (Discovery RGPIN-2015-05512, Discovery RGPIN-2014-04235, and CGS-M to S.S.) and the Canada Research Chairs program in Advanced Cellular Microenvironments to C.M. and in Biocolloids and Surfaces to N.T. We would like to thank

DOI: 10.1021/acs.langmuir.9b00803
Langmuir XXXX, XXX, XXX−XXX

Wontae Lee for help in performing shear rheology measurements and the Department of Chemical Engineering/Eugenie Ulmer Lamothe graduate student fellowship fund for support to S.S.

REFERENCES

(1) Hetrick, E. M.; Schoenfisch, M. H. Reducing implant-related infections: active release strategies. *Chem. Soc. Rev.* **2006**, *35*, 780−789.
(2) Kasemo, B.; Gold, J. Implant Surfaces and Interface Processes. *Adv. Dent. Res.* **1999**, *13*, 8−20.
(3) Lill, H.; Hepp, P.; Korner, J.; Kassi, J. P.; Verheyden, A. P.; Josten, C.; Duda, G. N. Proximal humeral fractures: how stiff should an implant be? A comparative mechanical study with new implants in human specimens. *Arch. Orthop. Trauma Surg.* **2003**, *123*, 74−81.
(4) Wang, X.; Xu, S.; Zhou, S.; Xu, W.; Leary, M.; Choong, P.; Qian, M.; Brandt, M.; Xie, Y. M. Topological design and additive manufacturing of porous metals for bone scaffolds and orthopaedic implants: A review. *Biomaterials* **2016**, *83*, 127−141.
(5) Ramakrishna, S.; Mayer, J.; Wintermantel, E.; Leong, K. W. Biomedical applications of polymer-composite materials: a review. *Compos. Sci. Technol.* **2001**, *61*, 1189−1224.
(6) Barnes, J. M.; Przybyla, L.; Weaver, V. M. Tissue mechanics regulate brain development, homeostasis and disease. *J. Cell. Sci.* **2017**, *130*, 71−82.
(7) Handorf, A. M.; Zhou, Y.; Halanski, M. A.; Li, W. J. Tissue stiffness dictates development, homeostasis, and disease progression. *Organogenesis* **2015**, *11*, 1−15.
(8) Cox, T. R.; Erler, J. T. Remodeling and homeostasis of the extracellular matrix: implications for fibrotic diseases and cancer. *Dis. Models & Mech.* **2011**, *4*, 165−178.
(9) Spencer, K. C.; Sy, J. C.; Ramadi, K. B.; Graybiel, A. M.; Langer, R.; Cima, M. J. Characterization of Mechanically Matched Hydrogel Coatings to Improve the Biocompatibility of Neural Implants. *Sci. Rep.* **2017**, *7*, No. 1952.
(10) Costerton, J. W.; Montanaro, L.; Arciola, C. R. Biofilm in implant infections: Its production and regulation. *J. Artif. Organs* **2005**, *28*, 1062−1068.
(11) O'Toole, G.; Kaplan, H. B.; Kolter, R. Biofilm Formation as Microbial Development. *Annu. Rev. Microbiol.* **2000**, *54*, 49−79.
(12) Hall-Stoodley, L.; Costerton, J. W.; Stoodley, P. Bacterial biofilms: from the natural environment to infectious diseases. *Nat. Rev. Microbiol.* **2004**, *2*, 95−108.
(13) Costerton, J. W.; Stewart, P. S.; Greenberg, E. P. Bacterial Biofilms: A Common Cause of Persistent Infections. *Science* **1999**, *284*, 1318.
(14) Garrett, T. R.; Bhakoo, M.; Zhang, Z. Bacterial adhesion and biofilms on surfaces. *Prog. Nat. Sci.* **2008**, *18*, 1049−1056.
(15) Hall-Stoodley, L.; Stoodley, P. Evolving concepts in biofilm infections. *Cell Microbiol.* **2009**, *11*, 1034−1043.
(16) Normark, B. H.; Normark, S. Evolution and spread of antibiotic resistance. *J. Intern. Med.* **2002**, *252*, 91−106.
(17) Andersson, D. I. Persistence of antibiotic resistant bacteria. *Curr. Opin. Microbiol.* **2003**, *6*, 452−456.
(18) Høiby, N.; Bjarnsholt, T.; Givskov, M.; Molin, S.; Ciofu, O. Antibiotic resistance of bacterial biofilms. *Int. J. Antimicrob. Agents* **2010**, *35*, 322−332.
(19) Andersson, D. I.; Hughes, D. Antibiotic resistance and its cost: is it possible to reverse resistance? *Nat. Rev. Microbiol* **2010**, *8*, 260−271.
(20) Czaplewski, L.; Bax, R.; Clokie, M.; Dawson, M.; Fairhead, H.; Fischetti, V. A.; Foster, S.; Gilmore, B. F.; Hancock, R. E. W.; Harper, D.; Henderson, I. R.; Hilpert, K.; Jones, B. V.; Kadioglu, A.; Knowles, D.; Ólafsdóttir, S.; Payne, D.; Projan, S.; Shaunak, S.; Silverman, J.; Thomas, C. M.; Trust, T. J.; Warn, P.; Rex, J. H. Alternatives to antibiotics—a pipeline portfolio review. *Lancet Infect. Dis.* **2016**, *16*, 239−251.
(21) Song, F.; Koo, H.; Ren, D. Effects of Material Properties on Bacterial Adhesion and Biofilm Formation. *J. Dent. Res.* **2015**, *94*, 1027−1034.
(22) Epstein, A. K.; Hochbaum, A. I.; Kim, P.; Aizenberg, J. Control of bacterial biofilm growth on surfaces by nanostructural mechanics and geometry. *Nanotechnology* **2011**, *22*, No. 494007.
(23) Schneider, A.; Francius, G.; Obeid, R.; Schwinte, P.; Hemmerlé, J.; Frisch, B.; Schaaf, P.; Voegel, J.-C.; Senger, B.; Picart, C. Polyelectrolyte Multilayers with a Tunable Young's Modulus: Influence of Film Stiffness on Cell Adhesion. *Langmuir* **2006**, *22*, 1193−1200.
(24) Moraes, C.; Sun, Y.; Simmons, C. A. (Micro)managing the mechanical microenvironment. *Integr. Biol.* **2011**, *3*, 959−971.
(25) Discher, D. E.; Janmey, P.; Wang, Y.-l. Tissue cells feel and respond to the stiffness of their substrate. *Science* **2005**, *310*, 1139−1143.
(26) Wells, R. G. The role of matrix stiffness in regulating cell behavior. *Hepatology* **2008**, *47*, 1394−1400.
(27) Teughels, W.; Van Assche, N.; Sliepen, I.; Quiryen, M. Effect of material characteristics and/or surface topography on biofilm development. *Clin. Oral Imp. Res.* **2006**, *17*, 68−81.
(28) Guégan, C.; Garderes, J.; Le Pennec, G.; Gaillard, F.; Fay, F.; Linossier, I.; Herry, J. M.; Fontaine, M. N.; Rehel, K. V. Alteration of bacterial adhesion induced by the substrate stiffness. *Colloids Surf., B* **2014**, *114*, 193−200.
(29) Kolewe, K. W.; Peyton, S. R.; Schiffman, J. D. Fewer Bacteria Adhere to Softer Hydrogels. *ACS Appl. Mater. Interfaces* **2015**, *7*, 19562−19569.
(30) Lichter, J. A.; Thompson, M. T.; Delgadillo, M.; Nishikawa, T.; Rubner, M. F.; Van Vliet, K. J. Substrata mechanical stiffness can regulate adhesion of viable bacteria. *Biomacromolecules* **2008**, *9*, 1571−1578.
(31) Song, F.; Ren, D. Stiffness of cross-linked poly-(dimethylsiloxane) affects bacterial adhesion and antibiotic susceptibility of attached cells. *Langmuir* **2014**, *30*, 10354−10362.
(32) Wang, Y.; Guan, A.; Isayeva, I.; Vorvolakos, K.; Das, S.; Li, Z.; Phillips, K. S. Interactions of Staphylococcus aureus with ultrasoft hydrogel biomaterials. *Biomaterials* **2016**, *95*, 74−85.
(33) Lu, H.; Koo, L. Y.; Wang, W. M.; Lauffenburger, D. A.; Griffith, L. G.; Jensen, K. F. Microfluidic Shear Devices for Quantitative Analysis of Cell Adhesion. *Anal. Chem.* **2004**, *76*, 5257−5264.
(34) Ng, J. M. K.; Gitlin, I.; Stroock, A. D.; Whitesides, G. M. Components for integrated poly (dimethylsiloxane) microfluidic systems. *Electrophoresis* **2002**, *23*, 3461−3473.
(35) Whitesides, G. M. The origins and the future of microfluidics. *Nature* **2006**, *442*, 368−373.
(36) Andersson, H.; van den Berg, A. Microfluidic devices for cellomics: a review. *Sens. Actuators, B* **2003**, *92*, 315−325.
(37) Inamdar, N. K.; Borenstein, J. T. Microfluidic cell culture models for tissue engineering. *Curr. Opin. Biotechnol.* **2011**, *22*, 681−689.
(38) El-Ali, J.; Sorger, P. K.; Jensen, K. F. Cells on chips. *Nature* **2006**, *442*, 403−411.
(39) Moraes, C.; Kagoma, Y. K.; Beca, B. M.; Tonelli-Zasarsky, R. L.; Sun, Y.; Simmons, C. A. Integrating polyurethane culture substrates into poly(dimethylsiloxane) microdevices. *Biomaterials* **2009**, *30*, 5241−5250.
(40) Moraes, C.; Labuz, J. M.; Shao, Y.; Fu, J.; Takayama, S. Supersoft lithography: candy-based fabrication of soft silicone microstructures. *Lab. Chip.* **2015**, *15*, 3760−3765.
(41) Rao, L.; Zhou, H.; Li, T.; Li, C.; Duan, Y. Y. Polyethylene glycol-containing polyurethane hydrogel coatings for improving the biocompatibility of neural electrodes. *Acta Biomater.* **2012**, *8*, 2233−2242.
(42) Lu, Y.; Wang, D.; Li, T.; Zhao, X.; Cao, Y.; Yang, H.; Duan, Y. Y. Poly(vinyl alcohol)/poly(acrylic acid) hydrogel coatings for improving electrode-neural tissue interface. *Biomaterials* **2009**, *30*, 4143−4151.

DOI: 10.1021/acs.langmuir.9b00803
Langmuir XXXX, XXX, XXX−XXX

(43) Young, E. W.; Wheeler, A. R.; Simmons, C. A. Matrix-dependent adhesion of vascular and valvular endothelial cells in microfluidic channels. *Lab. Chip.* **2007**, *7*, 1759−1766.
(44) Busscher, H. J.; van der Mei, H. C. Microbial adhesion in flow displacement systems. *Clin. Microbiol. Rev.* **2006**, *19*, 127−141.
(45) Katsikogianni, M.; Missirlis, Y. F. Concise review of mechanisms of bacterial adhesion to biomaterials and of techniques used in estimating bacteria-material interactions. *Eur. Cells Mater.* **2004**, *8*, 37−57.
(46) Duddridge, J. E.; Kent, C. A.; Laws, J. F. Effect of surface shear stress on the attachment of *Pseudomonas fluorescens* to stainless steel under defined flow conditions. *Biotechnol. Bioeng.* **1982**, *24*, 153−164.
(47) Dickinson, R. B.; Cooper, S. L. Analysis of Shear-Dependent Bacterial Adhesion Kinetics to Biomaterial Surfaces. *AIChE J.* **1995**, *41*, 2160−2174.
(48) Isberg, R. R.; Barnes, P. Dancing with the Host: Flow-Dependent Bacterial Adhesion. *Cell* **2002**, *110*, 1−4.
(49) Bos, R.; van der Mei, H. C.; Busscher, H. J. Physico-chemistry of initial microbial adhesive interactions. *FEMS Microbiol. Rev.* **1999**, *23*, 179−230.
(50) Abu-Lail, N. I.; Camesano, T. A. Role of Lipopolysaccharides in the Adhesion, Retention, and Transport of Escherichia coli JM109. *Environ. Sci. Technol.* **2003**, *37*, 2173−2183.
(51) Dunne, W. M. Bacterial Adhesion: Seen Any Good Biofilms Lately? *Clin. Microbiol. Rev.* **2002**, *15*, 155−166.
(52) Woods, D. E.; Straus, D. C.; Johanson, W. G.; Bass, J. A. Role of Fibronectin in the Prevention of Adherence of Pseudomonas aeruginosa to Buccal Cells. *J. Infect. Dis.* **1981**, *143*, 784−790.
(53) Vercellotti, G. M.; McCarthy, J. B.; Lindholm, P.; Peterson, P. K.; Jacob, H. S.; Furcht, L. T. Extracellular Matrix Proteins (Fibronectin, Laminin, and Type IV Collagen) Bind and Aggregate Bacteria. *Am. J. Pathol.* **1985**, *120*, 13−21.
(54) van Loosdrecht, M. C. M.; Norde, W.; Lyklema, J.; Zehnder, A. J. B. Hydrophobic and electrostatic parameters in bacterial adhesion. *Aquat. Sci.* **1990**, *52*, 103−114.
(55) Abraham, S. N.; Beachey, E. H.; Simpson, W. A. Adherence of Streptococcus pyogenes, Escherichia coli, and Pseudomonas aeruginosa to Fibronectin-Coated and Uncoated Epithelial Cells. *Infect. Immun.* **1983**, *41*, 1261−1268.
(56) Xicohtencatl-Cortes, J.; Monteiro-Neto, V.; Saldana, Z.; Ledesma, M. A.; Puente, J. L.; Giron, J. A. The type 4 pili of enterohemorrhagic Escherichia coli O157:H7 are multipurpose structures with pathogenic attributes. *J. Bacteriol.* **2009**, *191*, 411−421.
(57) Hubble, J.; Ming, F.; Eisenthal, R.; Whish, W. Progressive Detachment of Cells from Surfaces: a Consequence of Heterogeneous Ligand Populations or a Multi-site Binding Equilibrium? *J. Theor. Biol.* **1996**, *182*, 169−171.
(58) Mohamed, N.; Rainier, T. R.; Ross, J. M. Novel Experimental Study of Receptor-Mediated Bacterial Adhesion Under the Influence of Fluid Shear. *Biotechnol. Bioeng.* **2000**, *68*, 628−636.

DOI: 10.1021/acs.langmuir.9b00803
Langmuir XXXX, XXX, XXX−XXX